Barbaraci, G., Virzì-Mariotti, G. Robust control for a suspended rotating shaft by radial active magnetic bearings. Balkan journal of Mechanical Transmissions, Volume 1 (2011), Issue 1, pp. 4-11, ISSN 2069–5497.

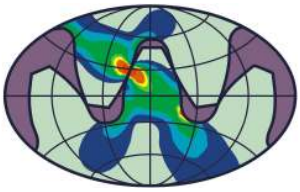

Balkan Association of Power Transmissions (BAPT)

Balkan Journal of Mechanical Transmissions

Volume 1 (2011), Issue 1, pp. 4-11
ISSN 2069–5497

ROmanian Association of MEchanical Transmissions (ROAMET)

ROBUST CONTROL FOR A SUSPENDED ROTATING SHAFT BY RADIAL ACTIVE MAGNETIC BEARINGS

Gabriele BARBARACI, Gabriele VIRZÌ MARIOTTI

ABSTRACT. *This paper shows a comparison based on dynamic behaviour of a rotating shaft when it is suspended by 4-axis active magnetic bearings under several control systems. The control systems used are μ-synthesis, loop shaping design procedure and Sub(H_∞) robust control with the introduction of uncertainties on position and current gains of the actuators. Each of these controllers is characterized by four input signals and four output signals and the introduction of uncertainties on displacement gain and current gain is due to torn and worn of the components during the time, which can lead the entire system to instability phenomena. The comparison of the performances is obtained through the introduction of same weighting function for all three control systems. All simulations and results are performed by MATLab.*

KEYWORDS. *Rigid rotor, active magnetic bearing, robust control.*

NOMENCLATURE

Symbol	Description
Ω	Angular speed of shaft
$\mathbf{q}_g(t)$	Vector of center of mass displacements
$\mathbf{q}_b(t)$	Vector of bearing section displacements
$\mathbf{q}_{sensor}(t)$	Vector of displacement captured by sensors
$\mathbf{B}_{\Theta mag}$	Transformation matrix of magnetic bearing force in the same direction of x_g and y_g
$\mathbf{B}_{mag}$	Transformation coordinates matrix of magnetic bearing force on center of mass of rotor
$\mathbf{B}_{\Theta disp}$	Transformation matrix of magnetic bearing force in the same direction of x_g and y_g
$\mathbf{B}_{sensor}$	Transformation coordinates of displacements of sensor and center of mass of shaft
α	Slope of magnets
$\mathbf{P}_{\mathbf{K}_S}$	Maximum percentage of $\mathbf{K}_S$ uncertainty
$\mathbf{P}_{\mathbf{K}_I}$	Maximum percentage of $\mathbf{K}_I$ uncertainty
$\mathbf{\Delta}_{\mathbf{K}_S}$	Range of $\mathbf{K}_S$ uncertainty
$\mathbf{\Delta}_{\mathbf{K}_I}$	Range of $\mathbf{K}_I$ uncertainty
$\mathbf{M}$	Mass matrix of the shaft
$\mathbf{G}$	Gyroscopic matrix of the shaft
$\mathbf{M_b}$	Mass matrix after the transformation coordinates
$\mathbf{G_b}$	Gyroscopic matrix after the transformation coordinate
$\mathbf{K}_S$	Matrix of displacement gain
$\mathbf{K}_I$	Matrix of current gain
$\mathbf{I}$	Identity matrix
$\mathbf{i}_c(t)$	Vector of control current
$\overline{\sigma}$	Structured singular value

1. INTRODUCTION

Active Magnetic Bearing (AMB) uses electromagnets to attract the ferromagnetic cape winding of the rotor which is free to rotate without physical contact with the bearing. (Schweitzer et al., 2009; Genta, 2005; Barbaraci et al., 200, 2010). This operation, called active magnetic levitation, is unstable unless of a certain control's algorithm performed respecting the imposed constraining. In order to achieve a stable levitation, an active feedback control of the current in the magnetic coils is necessary. As it might be expected, a variety of control schemes are used and a variety of studies have been done for AMB control. The dynamic system however depends above all on the rotor's angular speed because of the gyroscopic effect, as for any rotating dynamic system. The gyroscopic effect leads the system to instability phenomena which must be considered in order to achieve stable levitation. The rotor motion is characterized by translation along *x*-*y* directions and rotation of rotor around those axes. Moreover the transformation coordinates allows relating the displacements captured by the sensors and the displacements of the section located on the middle plane of the bearings. Without a suitable control system the magnetic levitation is not possible. During last twenty years a number of control systems are applied on magnetic levitation in order to provide enough acknowledge about the capability of rotor to maintain the contactless with the stator. Obviously there are many control systems which are not able to maintain the operating point position without a further algorithm such as the integrator of a PID controller, some other control system need the entire state vector to create the feedback such as the optimal control characterized by a matrix which number of columns is equal to the dimension of state vector. The cutting edge of control systems is represented by μ-synthesis, loop shaping design procedure and H-infinity robust control, this last with its variant sub$(H)_\infty$. The reason is not only about the recovering of operating point position without integrator but also the possibility to avoid the use of some sensors to capture further components belonging to the state vector, a problem that usually is solved by the introduction of a linear observer. In case of dynamic perturbations, the use of

robust control has the advantage to neglect: the non-linearity, the effects of reduced-order models, the change of system parameters due to environmental changes, hysteresis, torn and worn factors. Moreover it is used also in case of a sensor and actuator noise problem. An application of μ-synthesis controller was for the Army's weapon system. The test fixture is patterned after the Apache helicopter's 30 mm gun (Bugajski et al., 1993) and has tuneable nonlinearities which may be representative not only of the nonlinearities of the gun, but of other mechanical systems as well. The models of the test fixture that were available at the time of the work are also described. The goal in pointing the gun is to reduce dispersions of fired gun rounds on targets. The resulting μ-synthesis design, when connected with nonlinear simulation, exhibited limit-cycle behaviour of unacceptable amplitude. Due to high surface speed and active control capabilities, active magnetic bearings hold great promise for high speed machining spindles. The control problem given by this application is examined and the development of an advanced prototype is reviewed (Sawicki et al., 2007). A μ-synthesis framework is proposed for this problem and it is shown that the minimization of the susceptibility to machining chatter may be easily put into this framework. In addition to handling uncertainties in sensor and actuator components, this formulation may also include an uncertainty representing the range of cutting tools for the spindle (Knospe and Fittro, 1997). The proposed control algorithms are developed using μ-analysis to obtain robust stability and robust performance in the simulation; three different active control algorithms are used. A similar approach is applied where a comparison between three different controllers is performed in order to analyze the differences on the dynamic behaviour (Wu and Lin, 2005). Many other applications of robust control are performed through loop-shaping design procedure such were an H_∞ controller is performed by evolution optimization to control a robot arm. The loop shaping method is commonly used also to obtain the conditions of robust stability and robust performance. This technique is a particular optimization problem to guarantee closed loop stability at all frequencies (Kaitwanidvilai and Parnichkun, 2003).

Aim of the present study is to identify which type of control, among those taken into consideration, is best placed to achieve magnetic levitation for a rigid rotor and achieve both robust control and robust performance, once the weighting functions are introduced.

1.1 State of the Art

The first experiments on magnetic levitation dates back to 1937; but already in 1842 Earnshow showed that the permanent magnets are unable to achieve stable hovering for a body of ferromagnetic material and that the same body can achieve stable hovering only if the magnetic field is adjusted continuously in time. This can be achieved by automatically controlled electromagnets. The magnetic levitation vehicle (MAGLEV) built by Japanese companies, uses active magnetic levitation on the principle outlined above. With a mass of 122,000 kg, the electromagnets ensure the contactless allowing the MAGLEV vehicle to reach speeds of 622 km/h. The obtained benefits by using active magnetic bearings have conducted their applications on several areas such as applications in highly restricted environment; in fact, magnetic bearings can also be used if the introduction of lubricant is prohibited since the forces generated may also act through a thin wall that isolates the sterile environments from the contaminated ones (Hoshi et al., 2006). The major benefit appears to be the high accuracy of machining due to the high peripheral speed of rotation and high load capacity that the active magnetic bearings can achieve. Another important advantage is to control and the damping of the vibrations, and to obtain the desired dynamic behavior. The active magnetic bearing, therefore, represents one of the options to achieve the absence of contact and a chance to reach a sufficiently high speed of rotation and translation.

A short history and general discussion of the operation of an active magnetic bearing, as well as specific applications of active magnetic bearings, are enclosed in the paper of Kasarda (2000) in both commercial and research scenarios. Although magnetic suspension devices have been used in nonrotating scenarios such as magnetically levitated trains, only applications associated with rotating equipment are addressed. Commercial applications such as large turbomachinery (Field and Iannello, 1998) and small-scale turbomolecular pumps are discussed. Research applications, such as bearingless motors (Chiba et al., 1998), flywheels for energy storage [Ahrens et al., 1994), micro-machines (Bleuler et al., 1994), and biomedical applications (Allaire et al., 1994) are presented.

2. MATHEMATICAL MODEL

The particular configuration examined in this work considers a rotor with four degree of freedom with eight poles for each active magnetic bearing, having a slope of 45° with regard to horizontal direction so that the force's resultant supports the rotor along the *x* and *y* direction crossing the centre of mass and rotating around them as Fig. 1 shows.

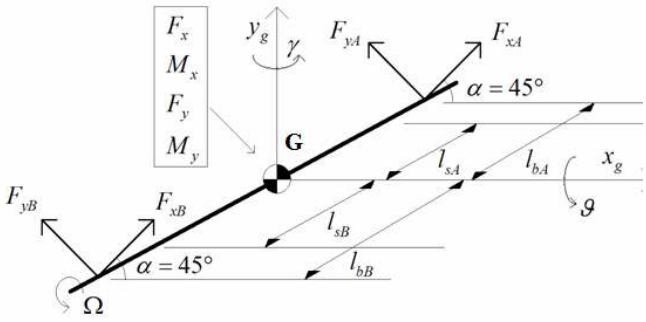

Fig. 1. Schematic view of 4-axis rotating shaft supported by two radial active magnetic bearings with sensors.

The system is subjected to a state of uncertainty about its displacement and current gain respectively $k_{(x,y)(A,B)}$ and $k_{(ix,iy)(A,B)}$ dictated by the parameters $\delta_{k_{(x,y)(A,B)},k_{(ix,iy)(A,B)}}$, in the range $P_{k_{(x,y)(A,B)},k_{(ix,iy)(A,B)}}$. The equation of motion is referred to the centre of gravity and it has the following expression:

$$\mathbf{M}\frac{d^2\mathbf{q}_g(t)}{dt^2}+\Omega\cdot\mathbf{G}\frac{d\mathbf{q}_g(t)}{dt}=\mathbf{B}_{\Theta mag}\mathbf{B}_{mag}\mathbf{f}(\mathbf{i}_c(t),\mathbf{q}_b(t)), \qquad (1)$$

By introducing the following transformation of coordinates:

$$\begin{cases} \mathbf{q}_b(t) = \mathbf{B}_{\Theta disp}\mathbf{B}_{mag}^{\mathbf{T}}\mathbf{q}_g(t) \\ \mathbf{q}_{sensor}(t) = \left(\mathbf{B}_{\Theta disp}\mathbf{B}_{sensor}\right)\left(\mathbf{B}_{\Theta disp}\mathbf{B}_{mag}^{\mathbf{T}}\right)^{-1}\mathbf{q}_b(t), \\ \mathbf{f}_{mag\_to\_g}(t) = \mathbf{B}_{\Theta mag}\mathbf{B}_{mag}\mathbf{f}(\mathbf{i}_c(t), \mathbf{q}_b(t)) \end{cases} \quad (2)$$

which considers the relation of the displacements between the section relative to bearing location and the sensors, the system is analyzed according to the equation of motion:

$$\mathbf{M}_b\frac{d^2\mathbf{q}_b(t)}{dt^2} + \Omega\cdot\mathbf{G}_b\frac{d\mathbf{q}_b(t)}{dt} = \mathbf{f}(\mathbf{i}_c(t), \mathbf{q}_b(t)), \quad (3)$$

The introduction of uncertainties on displacement gain and on current gain is used. The magnetic force produced by active magnetic bearings is linearized by Taylor's series expansion which leads to the expression of the force:

$$\begin{cases} \mathbf{f}(\mathbf{i_c}(t), \mathbf{q_b}(t)) \approx \mathbf{K_s}\mathbf{q_b}(t) + \mathbf{K_I}\mathbf{i_c}(t) \\ \mathbf{K_S} = \left(\overline{\mathbf{K}}_\mathbf{S} + \overline{\mathbf{K}}_\mathbf{S}\mathbf{P}_{\mathbf{K_S}}\Delta_{\mathbf{K_S}}\right) \in \mathbf{R}^{\mathbf{4\times4}} \\ \mathbf{K_I} = \left(\overline{\mathbf{K}}_\mathbf{I} + \overline{\mathbf{K}}_\mathbf{I}\mathbf{P}_{\mathbf{K_I}}\Delta_{\mathbf{K_I}}\right) \in \mathbf{R}^{\mathbf{4\times4}} \end{cases} \quad (4)$$

3. CONTROLLERS

In order to provide a stabilizing effect to control the position of the rotor, a suitable control system must be performed because no magnetic levitation can be stabilized without controller (Schweitzer et all, 1994, 2009). In this paper three different controller or rather loop shaping design, μ-synthesis and Sub(H_∞) robust control are performed according to the mathematical model (5) with the assumption (6);

$$\begin{cases} \begin{bmatrix}\dot{\mathbf{x}}_1(t)\\ \dot{\mathbf{x}}_2(t)\end{bmatrix} = \begin{bmatrix}\mathbf{0} & \mathbf{I}^{4\times4}\\ \left(\mathbf{M}_b^{-1}\overline{\mathbf{K}}_S\right)^{4\times4} & -\mathbf{M}_b^{-1}(\Omega\mathbf{G}_b)\end{bmatrix}\begin{bmatrix}\mathbf{x}_1(t)\\ \mathbf{x}_2(t)\end{bmatrix} + \\ + \begin{bmatrix}\mathbf{0} & \mathbf{0}^{4\times4}\\ \mathbf{P}_{\mathbf{K}_S}^{4\times4} & \mathbf{M}_b^{-1}\mathbf{P}_{\mathbf{K}_I}\end{bmatrix}\begin{bmatrix}\mathbf{u}_{\mathbf{K}_S}\\ \mathbf{u}_{\mathbf{K}_I}\end{bmatrix} + \begin{bmatrix}\mathbf{0}^{4\times4}\\ \overline{\mathbf{M}}_b^{-1}\overline{\mathbf{K}}_I\end{bmatrix}\mathbf{u}(t) \\ \begin{bmatrix}\mathbf{z}_1(t)\\ \mathbf{z}_2(t)\end{bmatrix} = \begin{bmatrix}\left(\mathbf{M}_b^{-1}\overline{\mathbf{K}}_S\right)^{4\times4} & \mathbf{0}\\ \mathbf{0} & \mathbf{0}^{4\times4}\end{bmatrix}\begin{bmatrix}\mathbf{x}_1(t)\\ \mathbf{x}_2(t)\end{bmatrix} + \begin{bmatrix}\mathbf{0}\\ \left(\mathbf{M}_b^{-1}\overline{\mathbf{K}}_I\right)^{4\times4}\end{bmatrix}\mathbf{u}(t) \\ \mathbf{y}(t)_{sensor} = \begin{bmatrix}\mathbf{I}^{4\times4} & \mathbf{0}^{4\times4}\end{bmatrix}\begin{bmatrix}\mathbf{x}_1^{\mathrm{T}}(t) & \mathbf{x}_2^{\mathrm{T}}(t)\end{bmatrix}^{\mathrm{T}} \end{cases} \quad (5)$$

$$\begin{cases} \mathbf{x}_1(t) = \begin{bmatrix}x_{bA}(t) & y_{bA}(t) & x_{bB}(t) & y_{bB}(t)\end{bmatrix}^{\mathbf{T}} \\ \mathbf{x}_2(t) = \begin{bmatrix}\dot{x}_{bA}(t) & \dot{y}_{bA}(t) & \dot{x}_{bB}(t) & \dot{y}_{bB}(t)\end{bmatrix}^{\mathbf{T}} \\ \mathbf{u}(t) = \mathbf{i}_c(t) \\ \begin{bmatrix}\mathbf{u}_{K_S}\\ \mathbf{u}_{K_I}\end{bmatrix} = \begin{bmatrix}\Delta_{\mathbf{K}_S} & \mathbf{0}^{4\times4}\\ \mathbf{0}^{4\times4} & \Delta_{\mathbf{K}_I}\end{bmatrix}\begin{bmatrix}\mathbf{z}_1(t)\\ \mathbf{z}_2(t)\end{bmatrix} \end{cases}, \quad (6)$$

For all kinds of robust control systems performed in this paper, a state space equation in a package form is built. The package form is characterized by the introduction of all inputs in terms of uncertainties, disturbances and control signal introduced into plant and all outputs as in (7) :

$$\mathbf{G} = \begin{bmatrix}\mathbf{A} & \mathbf{B}_1 & \mathbf{B}_2\\ \mathbf{C}_1 & \mathbf{D}_{11} & \mathbf{D}_{12}\\ \mathbf{C}_2 & \mathbf{D}_{21} & \mathbf{D}_{22}\end{bmatrix}, \quad (7)$$

where all matrices are the same present in the equations (5). The entire system (5) is expanded by the introductions of weighting functions which define the performances on position and force of the actuator and they have the expressions (8):

$$\begin{bmatrix}\mathbf{e}_p\\ \mathbf{e}_u\end{bmatrix} = \begin{bmatrix}\mathbf{W}_p(\mathbf{I}+\mathbf{GK})^{-1}\\ \mathbf{W}_u\mathbf{K}(\mathbf{I}+\mathbf{GK})^{-1}\end{bmatrix}\mathbf{d}, \quad (8)$$

where $\mathbf{e}_p$ and $\mathbf{e}_u$ are the output due to the disturbances **d.** The controller is robust if and only if the transfer function in (8) has $\|\ \|_\infty < 1$ for all possible uncertain transfer matrices $\mathbf{\Delta}$, in order to attenuate the effects of disturbances on position ***p*** and actuator ***u*** respectively.

The control system structure is a dynamic mathematical model having the following expression:

$$\begin{cases} \dot{\mathbf{x}}(t) = \mathbf{A}\mathbf{x}(t) + \mathbf{B}\mathbf{u}(t) \\ \mathbf{y}(t) = \mathbf{C}\mathbf{x}(t) \\ \mathbf{u}(t) = \mathbf{q}(t)_{sensor} \\ \mathbf{y}(t) = \mathbf{i}_c(t) \end{cases} \quad (9)$$

The way how the controllers are performed is characterized by different algorithm. In the case of mu-synthesis the algorithm implements the control system by reaching a mathematical condition:

$$\sup_{\omega\in\square}\inf_{\mathbf{D}\in\underline{\mathbf{D}}}\bar{\sigma}\left[\mathbf{DF}(\mathbf{G},\mathbf{K})\mathbf{D}^{-1}(j\omega)\right] < 1 \quad (10)$$

In particular once the plant of the system is known, the algorithm starts by an iterative calculation with new plant $\tilde{\mathbf{G}}$ as (11) once the open loop transfer function of system **F(G,K)** is known:

$$\tilde{\mathbf{G}} = \begin{bmatrix}\mathbf{D} & \mathbf{0}\\ \mathbf{0} & \mathbf{I}\end{bmatrix}\mathbf{G}\begin{bmatrix}\mathbf{D}^{-1} & \mathbf{0}\\ \mathbf{0} & \mathbf{I}\end{bmatrix} \quad (11)$$

where **D** is set as identity matrix for the first step. The controller is performed according the expression (12):

$$\mathbf{K} = \arg\inf_{\mathbf{K}}\left\|\mathbf{F}\left(\tilde{\mathbf{G}},\mathbf{K}\right)\right\|_\infty \quad (12)$$

so that a new matrix **D** is performed according the expression:

$$\mathbf{D}(j\omega) = \arg\inf_{\mathbf{D}\in\underline{\mathbf{D}}}\bar{\sigma}\left[\mathbf{DF}(\mathbf{G},\mathbf{K})\mathbf{D}^{-1}(j\omega)\right. \quad (13)$$

The iteration must be initialized until the condition expressed by (10) is achieved.

By a different algorithm, the Sub(H_∞) is performed where the first step is to solve the optimization problem for $\mathbf{K_0}$

expressed in (14) and computing the μ curve (15), corresponding to $\mathbf{K_0}$ over a chosen frequency range. The μ value must be normalized according to (16) and get the minimum phase of that.

$$\mathbf{K}_0 = \arg\inf_{\mathbf{K}} \left\| \mathbf{F}\left(\tilde{\mathbf{G}}, \mathbf{K}\right) \right\|_\infty \tag{14}$$

$$\mu_0\left(j\omega\right) = \mu\left[\mathbf{F}\left(\mathbf{G}, \mathbf{K}_0\right)\left(j\omega\right)\right] \tag{15}$$

$$\tilde{\mu}_0 = \frac{\mu_0}{\max_\omega \mu_0} \tag{16}$$

The control problem is solved by (17) and the iterative procedure must be repeated until a desired level of performance has been achieved.

$$\mathbf{K}_1 = \arg\inf_{\mathbf{K}} \left\| \tilde{\mu}_0 \mathbf{F}\left(\tilde{\mathbf{G}}, \mathbf{K}\right) \right\|_\infty \tag{17}$$

Algorithms are quite similar with each other. Totally different is the loop shaping design procedure algorithm, in fact the controller is performed according to condition (18):

$$\gamma = \min_{\mathbf{K}} \left\| \begin{bmatrix} \mathbf{I} \\ \mathbf{K} \end{bmatrix} \left(\mathbf{I} - \mathbf{GK}\right)^{-1} \begin{bmatrix} \mathbf{G} \\ \mathbf{I} \end{bmatrix} \right\|_\infty \geq 1 \tag{18}$$

In the expression (9) the iterative calculation is based on reaching the **K** dynamic control system respecting the condition on γ value. In all control system, **G** takes in account the plant of the system and the weighting functions for required performance.

Table I: Data for the simulations

Symbol	Description	S.I.
m	Mass of rotor	$2.3Kg$
I_P	Polar moment of inertia	$8\times10^{-4} Kg\cdot m^2$
I_T	Transverse moment of inertia	$6\times10^{-2} Kg\cdot m^2$
l_{bA}	Distance bearing A from centre of mass	$0.241m$
l_{bB}	Distance bearing B from centre of mass	$0.139m$
l_{sA}	Distance sensor A from centre of mass	$0.241m$
l_{sB}	Distance sensor B from centre of mass	$0.119m$
α	Slope of bearings axis	45°
$P_{k_{(x,y)(A,B)}, k_{(ix,iy)(A,B)}}$	Uncertainties percentage	10%
$\delta_{k_{(x,y)(A,B)}, k_{(ix,iy)(A,B)}}$	Range of uncertainties	$[-1,1]$
$\bar{k}_{(x,y)(A,B)}$	Nominal displacement gain	$144000N/m$
$\bar{k}_{(ix,iy)(A,B)}$	Nominal current gain	$38N/A$

4. SIMULATIONS

The simulations are performed by considering the data contained in the table 1. Another set of data is referred to the transfer functions introduced in the plant of our system. These transfer functions are essential if a certain performance must be obtained; these performances are usually referred in the frequency domain.

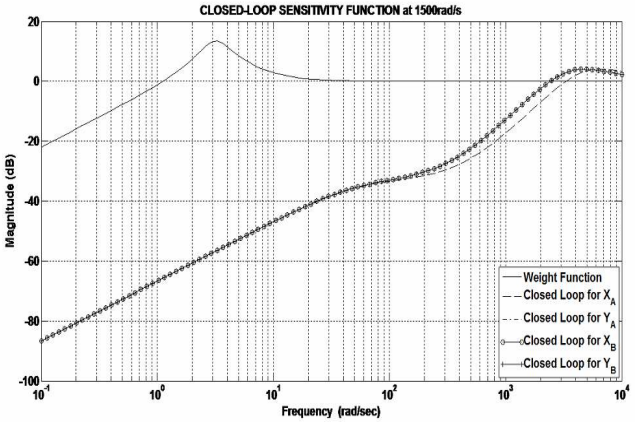

Fig. 2. Sensitivity functions describing how the disturbance affects the displacement with LSDP controller.

Figures 3 and 4 show that μ-synthesis and Sub(H_∞) robust control are not able to maintain good rejection of disturbances for the entire required range of frequency:

This work introduces a transfer function in the displacement output signal. The introduction of transfer function in Laplace domain "s" means that the displacement must be characterized by a certain dynamic behaviour according to the frequency variable. This technique is commonly used when a flexible structure is taken into account or when some nodes are subjected to vibrations such as in this case.

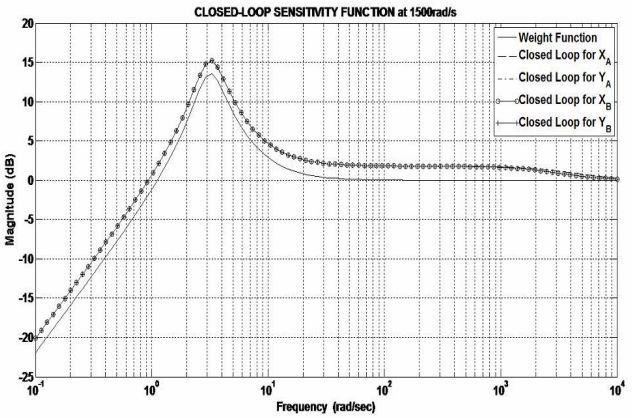

Fig. 3. Sensitivity function describing how the disturbance affects the displacement with μ-synthesis controller.

Figures 2, 3 and 4 show the frequency response of weighting function to the displacement performances in order to analyze the sensitivity function or the disturbances can affect the dynamic response of the system. This is made for all controlled axis of each radial active magnetic bearing. Figure 2 shows the sensitivity function for the loop shaping controller design; the system has a good attenuation of disturbances until a certain value of

frequency at 2×10^3 rad/s in dependence on the controlled axis:

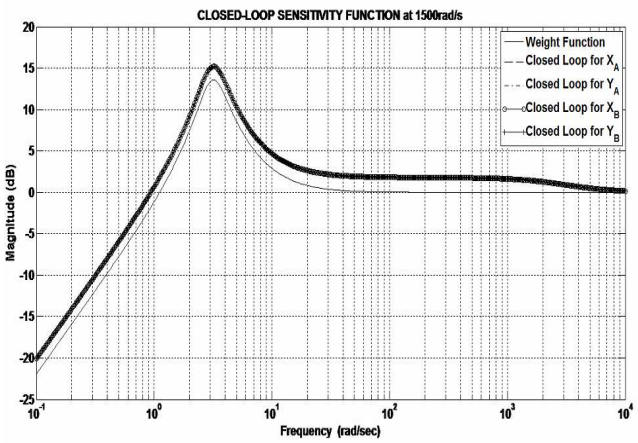

Fig. 4. Sensitivity function describing how the disturbance affects the displacement with Sub(H_∞) controller.

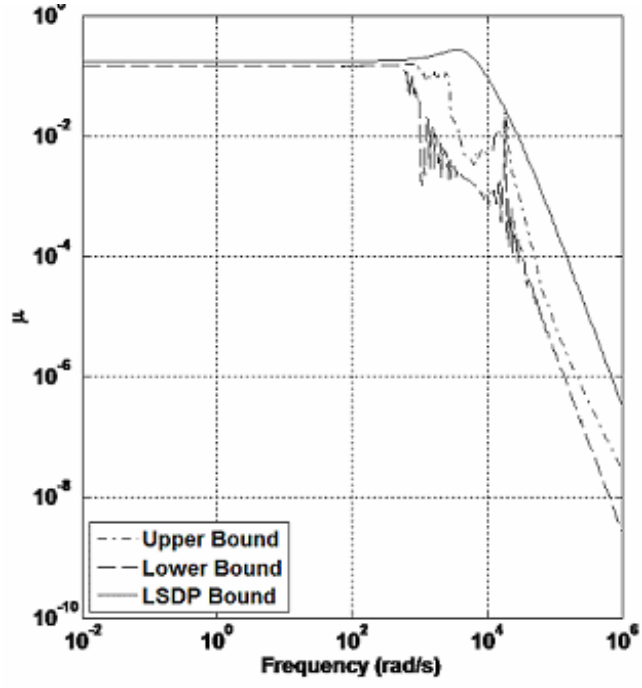

Fig. 5. Robust stability described by μ-value with LSDP controller.

Figure 5 shows the robust stability condition for loop shaping design procedure: the system has robust stability for all value of frequencies (upper and lower bound). The loop shaping design shows good performances until 10^3 rad/s for upper and lower bound and nominal plant as well (Fig. 6).

Figure 7 shows that robust stability for the μ-synthesis is well maintained for all values of frequencies but the same thing can not be said about the performances of it, in fact, for both nominal and perturbed systems the performances are low since μ<1. The same behavior is followed by the Sub(H_∞) control.

The simulations are performed at constant value of angular speed of 1500 rad/s in order to analyze the differences between the three controllers; figures 11 and 12 show respectively, the disturbances rejection and tracking of references analysis.

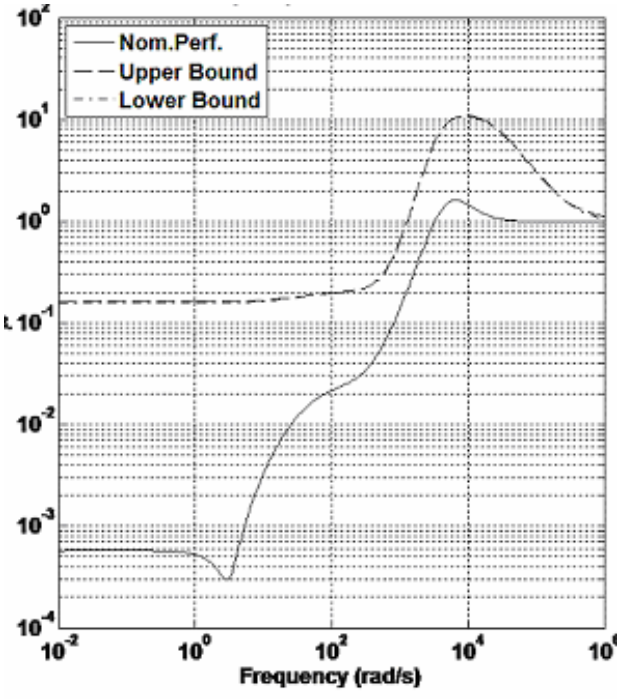

Fig.6. Nominal and robust performance function described by μ-value with LSDP controller.

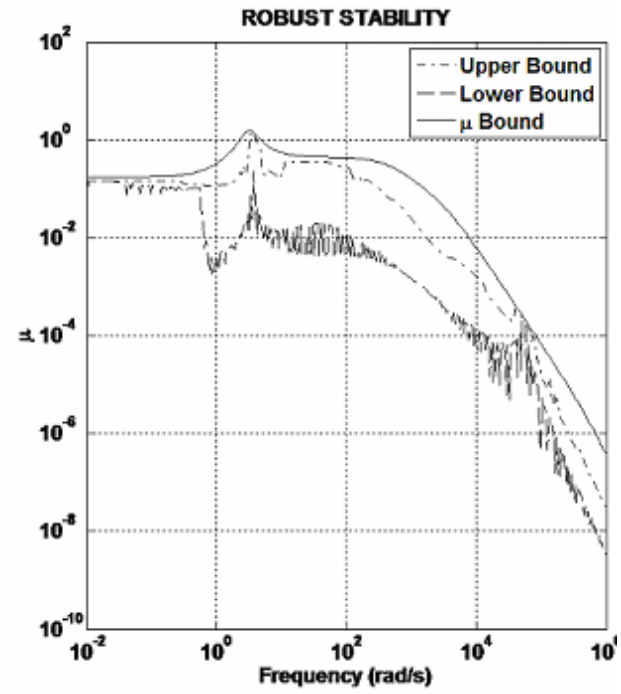

Fig.7. Robust stability by μ-value with μ-Synthesis

Figures 11 and 12 show that the disturbance rejection test is performed according to a simulation characterized by a range of time of sixty seconds and a disturbance injection built as a square wave (black line) with a period of 20*s* and an amplitude of $10^{-6}m$. All three implemented controllers are capable to support the requirements to reject the disturbance but their way of work is different.

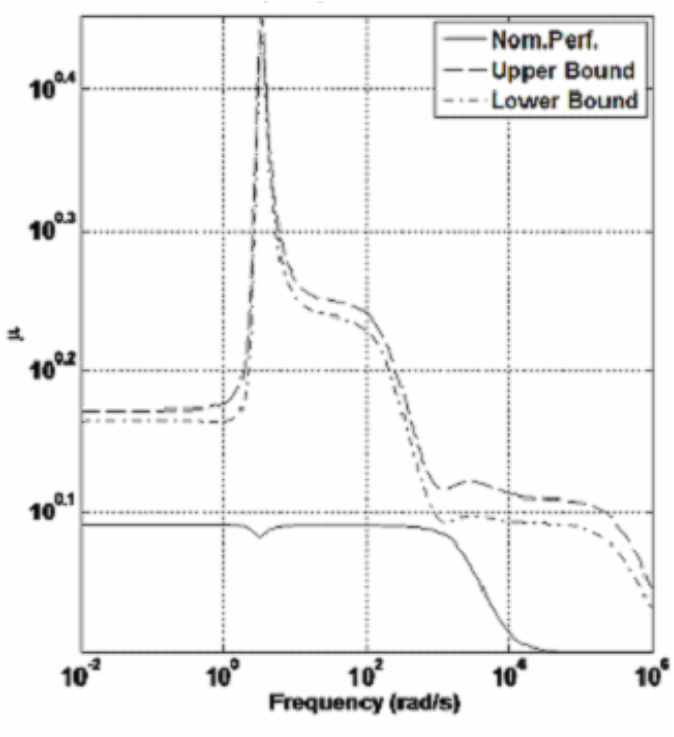

Fig. 8. Nominal and robust performance function described by μ-value with μ-Synthesis.

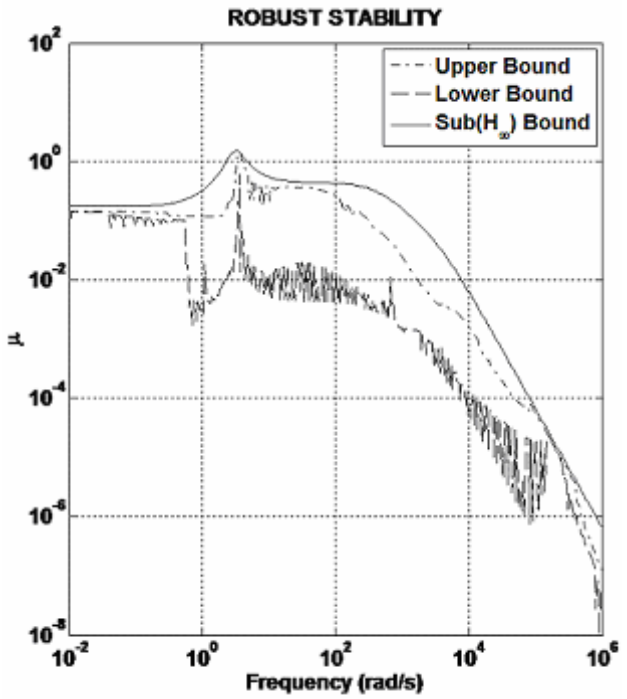

Fig. 9: Robust stability described by μ-value with Sub(H_∞).

The controllers Sub(H_∞) and μ-Synthesis are characterized by the same pattern, the same period of oscillation and they are perfectly superimposed. Their dynamic behavior is typical of damped systems where a certain overshoots value is present and different by the successive controller. The loop-shaping controller (red line) provides good performances for the disturbance rejection due to the short period to extinct the transient response and small overshoots value if compared with those offered by the previous controllers.

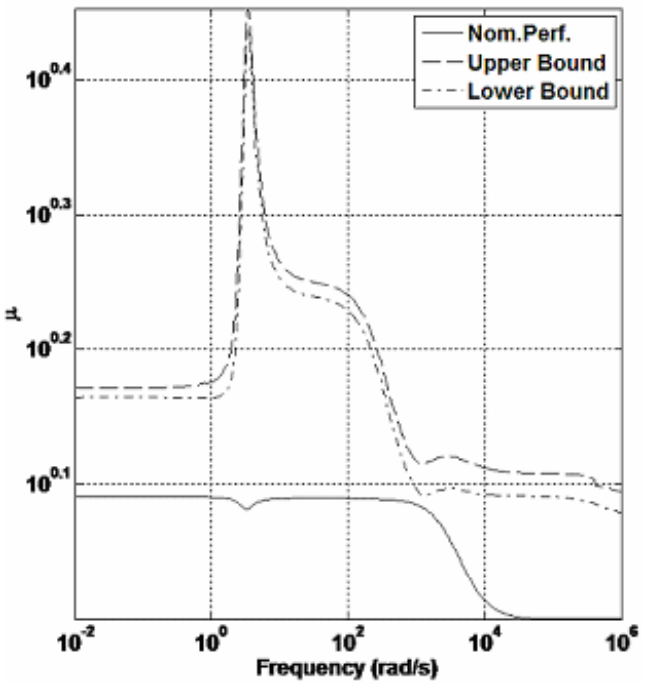

Fig. 10: Nominal and robust performance function described by μ-value with Sub(H_∞).

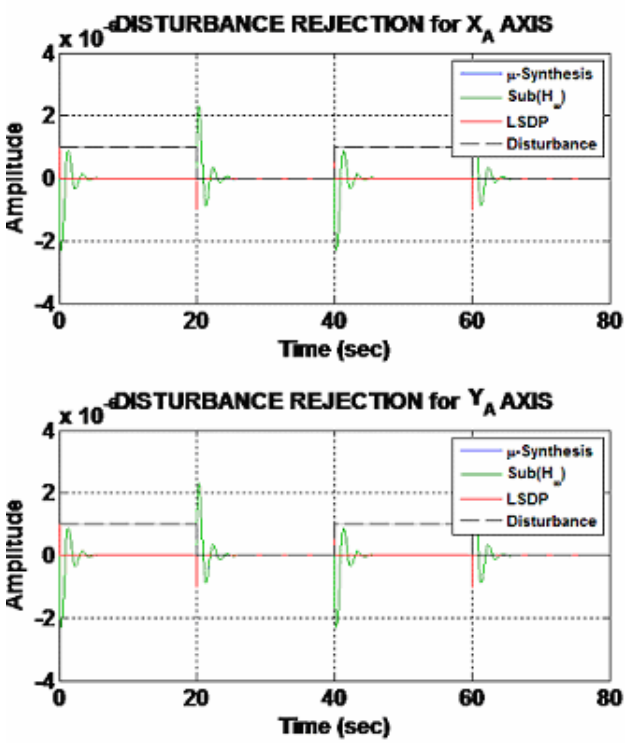

Fig. 11. Comparison via simulation for disturbance rejection on section A of the shaft

In all cases the controllers are able to reject the disturbances by leading all suspended section to maintain the operating point position. Figures 13 and 14 show the reference's tracking simulations. The input signals to analyze the behavior are the same of the disturbance rejection one but in this case the position of each suspended section must follow the input signals because the system must be able to adapt itself at every desired condition required by the user. Also in this case Sub(H_∞) and μ-Synthesis have the same

behavior, while loop-shaping has the best response due to the short settling time and small overshoot.

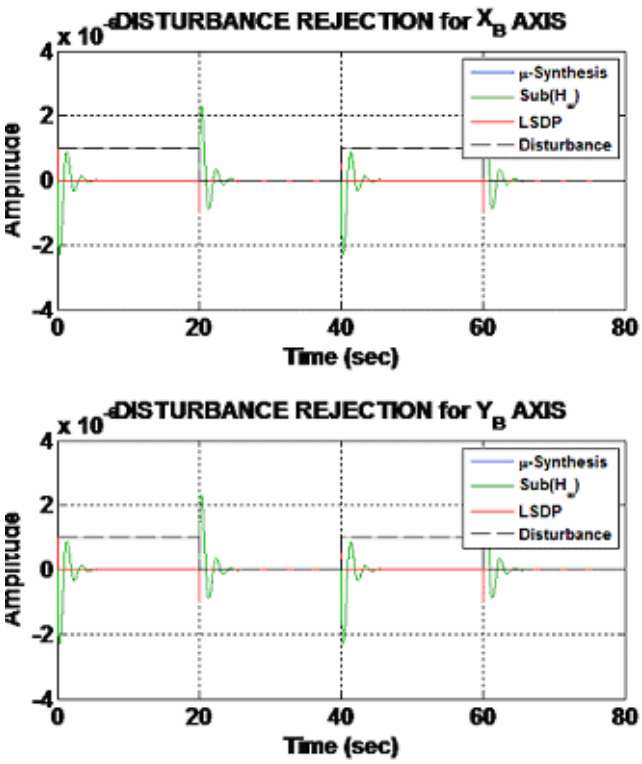

Fig. 12. Comparison via simulation for disturbance rejection on section B of the shaft.

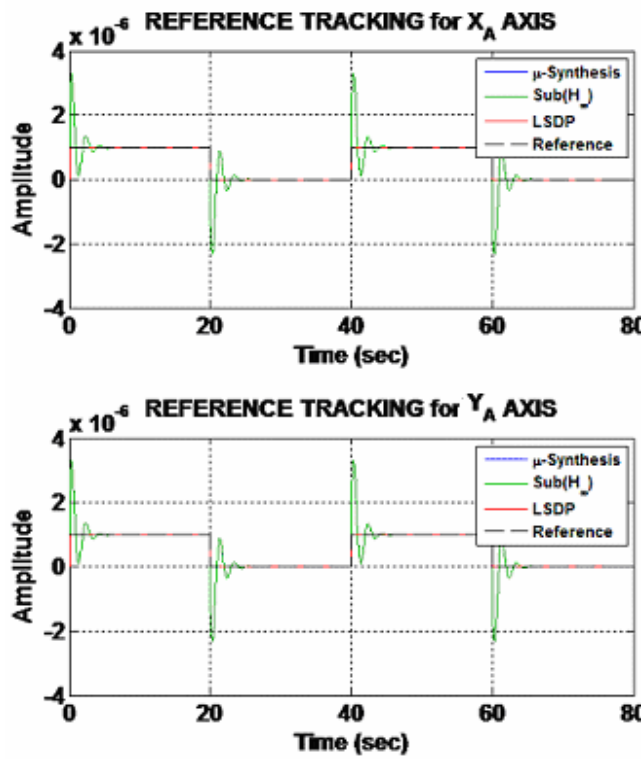

Fig.13. Comparison via simulation for reference tracking on section A for the shaft.

5. CONCLUSIONS

This paper shows a comparison among three different control systems for a suspended rotor by active magnetic bearings under the assumption that the rotor is rigid.

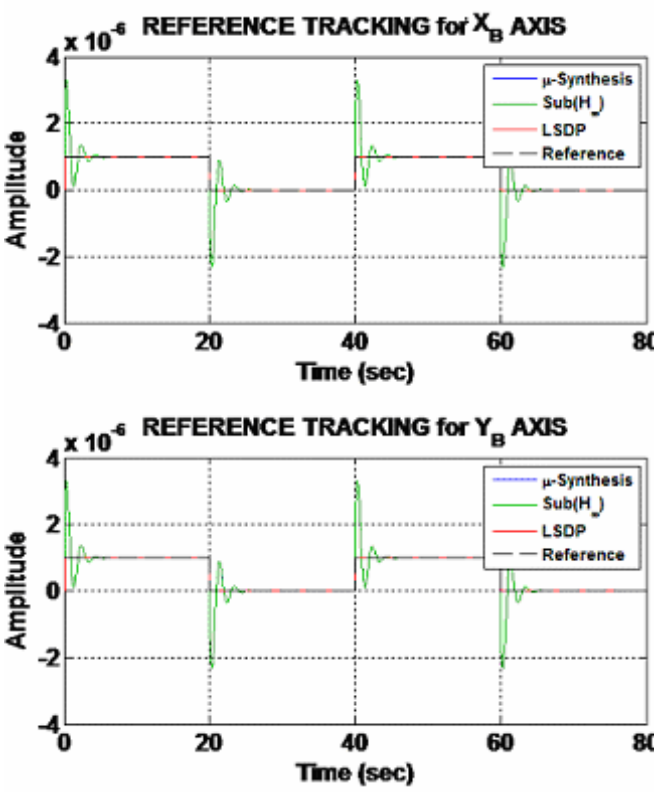

Fig. 14. Comparison via simulation for reference tracking on section B of the shaft.

The comparison shows that loop-shaping design procedure provides the best performance to eliminate the disturbances and to follow the reference's tracking when a certain performance is required on position and control current. The present study shows that once the weighting functions are introduced only the loop shaping design procedure is able to implement the system with robust stability and robust performance but all three control systems are able to suspend the rotor for magnetic levitation. As result of this analysis both the μ-synthesis and Sub(H∞) controllers show the same dynamic behavior when the rotor is subjected to the injection of the current. Their dynamic behavior is characterized by periodic oscillation with a settling time higher than that of loop shaping design, which is more ready in the response.

ACKNOWLEDGEMENTS

Authors thank Miss Giuseppina Dazzi for the improvement of the English language.

REFERENCES

AHRENS, M., TRAXLER, A., BURG, P. V., SCHWEITZER, G.. (1994). Design of a Magnetically Suspended Flywheel Energy Storage Device, Fourth International Symposium on Magnetic Bearings, Zurich, pp. 553-558.

ALLAIRE, P. E., MASLEN, E. H., KIM, H. C., BEARNSON, G. B., OLSEN, D.B. (1996). Design of a magnetic bearing-supported prototype centrifugal artificial heart pump, Tribology Transactions, 39 (3), pp. 663-669.

BARBARACI, G., PESCH, A. H., SAWICKI, J. T. (2010).

Experimental investigation of minimum power consumption optimal control for variable speed AMB rotor. In Proceedings of the ASME 2010 International Mechanical Engineering Congress & Exposition IMECE2010, Vancouver, British Columbia, pp. 1-10,

BARBARACI, G., VIRZÌ MARIOTTI, G. (2009). Controllo Subottimo per un Albero Rotante in Levitazione Magnetica Attiva, XXXVIII convegno nazionale AIAS, 9-11 Settembre 2009, Torino, Italy.

BLEULER, H., KAWAKATSU, H., TANG, W., HSIEH, W., MIU, D., TAI, Y., MOESNER, F., ROHNER, M. (1994). Micromachined Active Magnetic Bearings, Fourth International Symposium on Magnetic Bearings, pp. 349-352. Zurich.

BUGAJSKI, D., ENNS, D., TANNENBAUM, A. (1993). Synthesis methods for robust nonlinear control American Control Conference, pp. 531-535.

CHIBA, A., YOSHIDA, K., TADASHI, F. (1998). Transient Response of Revolving Magnetic Field in Induction Type Bearingless Motors with Secondary Resistance Variations. Sixth International Symposium on Magnetic Bearings, pp. 461-475. Cambridge, Massachusetts.

CLARK, A. (6/6/2005). "China's 270mph flying train could run on London to Glasgow route if plan takes off". The Guardian http://www.guardian.co.uk/uk/2005/jun/06/communities.china. Retrieved 26 December 2008.

EARNSHAW, S. (1842). On the Nature of the Molecular Forces Which Regulate the Constitution of the Luminferous Ether., Trans. Camb. Phil. Soc., 7, pp. 97-112

FIELD, R. J., IANNELLO, V. (1998). A Reliable Magnetic Bearing System for Turbomachinery, Sixth International Symposium on Magnetic Bearings, Cambridge, Massachusetts, pp. 42-51.

GENTA, G. (2005). Dynamics of Rotating Systems, Springer editions, Mechanical Engineering Series, Torino.

HOSHI H., SHINSHI T., TAKATANI S. (2006). Third-generation Blood Pumps With Mechanical Noncontact Magnetic Bearings. Artificial Organs, Vol. 30, Number 5, pp. 324–338,

KAITWANIDVILAI, S., PARNICHKUN, M. (2003). Design of Structured Controller Satisfying H_∞ Loop Shaping using Evolutionary Optimization: Application to a Pneumatic Robot Arm, Engineering Letters, 16:2, EL_16_2_03.

KASARDA, M. E. F. (2000). Overview of active magnetic bearing technology and applications, Shock and Vibration Digest Volume 32, Number 2, pp. 91-99

KNOSPE, C.R., FITTRO, R.L. (1997). Control of a High Speed Machining Spindle via μ-Synthesis, Proceedings of the 1997 IEEE International Conference on Control Applications Hartford, CT, October 5-7, 1997.

MAAS, H. Schanghai stutzt den Transrapid (in German). Tagesspiegel. http://www.tagesspiegel.de/wirtschaft/Transrapid-China; art271,2448347. Retrieved 27 March 2008.

SAWICKI J. T., MASLEN E. H.,. BISCHOF K. R. (2007). Modelling and performance evaluation of machining spindle with active magnetic bearings. Journal of Mechanical Science and Technology, Volume 21, Number 6, pp. 847-850.

SCHWEITZER, G., BLEULER, H., TRAXLER, A. (1994). Active Magnetic Bearings - Basics, Properties and Applications. vdf Hochschulverlag AG, ETH Zürich, 1994 (sold out). Author's Reprint, Zurich 2003.

SCHWEITZER, G., MASLEN, E. H. (2009). Magnetic Bearings: Theory, Design and Application to Rotating Machinery. Springer Editions, Zurich,.

WU, J. D., LIN, J. H. (2005). Implementation of an active vibration controller for gear-set shaft using μ-analysis, Journal of Sound and Vibration. Volume 281, Issues 3-5, pp. 1037–1055.

CORRESPONDENCE

Gabriele BARBARACI, Dr.
University of Palermo
Dipartimento di Ingegneria Chimica, Gestionale, Informatica e Meccanica
ED.8 Viale delle Scienze
90128 Palermo, Italia
barbaraci@dima.unipa.it

Gabriele VIRZÌ MARIOTTI, Prof.
University of Palermo
Dipartimento di Ingegneria Chimica, Gestionale, Informatica e Meccanica
ED.8 Viale delle Scienze
90128 Palermo, Italia
gabriele.virzìmariotti@unipa.it